arXiv:2004.01472v2 [cond-mat.stat-mech] 12 Aug 2020

$A + A \to \emptyset$ reaction for particles with a dynamic bias to move away from their nearest neighbour in one dimension

[1]**Reshmi Roy and** [2]**Parongama Sen**

[1,2] Department of Physics, University of Calcutta, 92 Acharya Prafulla Chandra Road, Kolkata 700009, India.

E-mail: [1]reshmi.roy80@gmail.com

Abstract. We consider the dynamics of particles undergoing the reaction $A+A \to \emptyset$ in one dimension with a dynamic bias. Here the particles move towards their nearest neighbour with probability $0.5 + \epsilon$ where $-0.5 \leq \epsilon < 0$. $\epsilon_c = -0.5$ is the deterministic limit where the nearest neighbour interaction is strictly repulsive. We show that the negative bias changes drastically the behaviour of the fraction of surviving particles $\rho(t)$ and persistence probability $P(t)$ with time t. $\rho(t)$ decays as $a/(\log t)^b$ where b increases with $\epsilon - \epsilon_c$. $P(t)$ shows a stretched exponential decay with non-universal decay parameters. The probability $\Pi(x,t)$ that a tagged particle is at position x from its origin is found to be Gaussian for all $\epsilon < 0$; the associated scaling variable is x/t^α where α approaches the known limiting value $1/4$ as $\epsilon \to \epsilon_c$, in a power law manner. Some additional features of the dynamics by tagging the particles are also studied. The results are compared to the case of positive bias, a well studied problem.

1. Introduction

Reaction diffusion systems have been extensively studied over the last few decades, especially in one dimension [1, 2, 3, 4, 5, 6, 7, 8, 9, 10, 11, 12, 13]. The simplest form of a reaction diffusion system is $A + A \to \emptyset$, where the particles A diffuse and annihilate on contact. This model in one dimension, with asynchronous updating, also represents the ordering dynamics of the Ising model with Glauber dynamics at zero temperature. When considered on a lattice, one can assume that the particles A occupy the sites of the lattice and at each time step they hop to a nearest neighbouring site.

The $A + A \to \emptyset$ system has been studied in the recent past where the particles A move with a bias towards their nearest neighbours [14, 15, 16] in one dimension. The model, in its deterministic limit, maps to a opinion dynamics model studied earlier [17]. Previously, both the bulk dynamical and tagged particle dynamics have been reported in the one dimensional $A+A \to \emptyset$ system where the particle A diffuses towards its nearest neighbour with a probability $0.5 + \epsilon$ $(0 < \epsilon \leq 0.5)$ and in the opposite direction with probability $0.5 - \epsilon$. The results show significant differences when compared to the case

with no bias ($\epsilon = 0$) although the annihilation process is identical in the latter. This reaction diffusion model with parallel updating has also been studied in two dimensions recently [18].

To generalize the problem, in the present paper, the results for a negative bias are reported, i.e., when $\epsilon < 0$. The idea behind the study is to find the universal behaviour in the bulk properties as well as the microscopic features. Here we have used asynchronous dynamics to compare with the positive bias case results which have already been studied before. Specifically, $\epsilon = -0.5$ implies purely repulsive motion where the particles always move towards their farther neighbour. These particles with full negative bias can represent the motion of similarly charged particles or in general particles with repulsive interaction which can move both ways. Henceforth we denote the fully biased point $\epsilon = -0.5$ by ϵ_c.

2. The Model, dynamics and simulation details

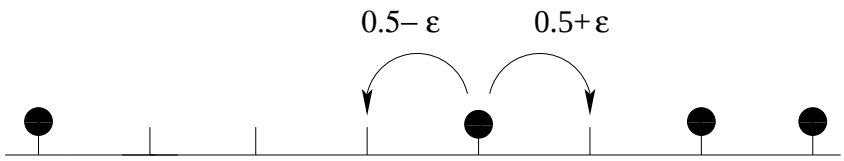


Figure 1. The tagged particle hops to right with probability $0.5 + \epsilon$ as its right neighbour is two lattice separation away and to left with probability $0.5 - \epsilon$ as the left neighbour is four lattice separation away. In the present case as $\epsilon < 0$, the particle has a preference to move in the left direction as its nearest neighbour is on its right. For $\epsilon = -0.5$, the particle definitely moves to the left. In comparison, in the conventional reaction diffusion case, $\epsilon = 0$ and the particle has equal probability to move left and right.

In the $A + A \to \emptyset$ model, a particle A diffuses to one of its neighbouring sites and undergoes a reaction (annihilation). Here, at each update, a site is randomly chosen and if there is a particle on the selected site, it hops one step towards its nearest neighbour with probability $0.5+\epsilon$ (and with probability $0.5-\epsilon$ in the opposite direction); $-0.5 \leq \epsilon < 0$. If the destination site is previously occupied by a particle, both of them will be annihilated simultaneously. The position of the particle is updated immediately in the asynchronous scheme of updating. L such updates constitute one Monte Carlo step (MCS). In the rare cases of two equidistant neighbours, the particle moves in either direction with equal probability 0.5. The motion is illustrated in figure 1. It may be noted that the direction of motion is determined by the relative distances of the neighbouring particles only; the particle has a tendency to move away from the nearest neighbour (for $\epsilon < 0$, which is the choice here). The actual distances are of no

consideration in the present scenario. Also, if a site is chosen for updating, the particle sitting at that site has to perform a move.

As asynchronous dynamics have been used, there are several interesting points to be noted. The net displacement of a particle can be zero or more than one after the completion of one MCS [16]. This affects the numerical estimates of certain quantities that have been estimated in the present work. For the fully biased point ϵ_c, annihilation can occur only if three particles occupy immediately adjacent sites, however, in the asynchronous update scheme, whether an annihilation will take place will depend on which site is getting updated first, so it is a necessary but not sufficient condition.

The studies are performed on lattices of maximum size $L = 24000$ and the maximum number of initial configurations taken is 2000. Periodic boundary condition has been used in all the simulations. We have considered the lattice of size L to be randomly half filled initially.

3. Simulation Results

We took snapshots of the system to check the motion of individual particles. The world lines of the motion of the particles are shown for $\epsilon = -0.1$ and -0.5 in figure 2. It may be noted immediately they are strikingly different from each other. It is obvious that the number of annihilation is larger for $\epsilon = -0.1$ and it is left with much fewer particles within the same timescale. Also, the paths traced out resemble more a diffusive trajectory. In contrast, for $\epsilon = -0.5$, the particles change their direction more often and remain confined within a limited region in space.

To probe the dynamics of the particles, we have studied the following quantities: (i) fraction of surviving particles $\rho(t)$ at time t, (ii) persistence probability of the lattice sites $P(t)$, (iii) the probability distribution $\Pi(x, t)$ of finding a particle A at distance x from its origin at time t, (iv) the probability $S(t)$ of the change in the direction in the motion of a particle at time t and (v) the distribution $D(\tau)$ of the time interval τ between two successive changes in the direction of the motion of a particle. The results for each of these quantities are presented in the following subsections.

3.1. Bulk properties

3.1.1. Fraction of surviving particles $\rho(t)$ For the purely diffusive system ($\epsilon = 0$), it is well known that the fraction of surviving particles shows a power law behaviour in time; $\rho(t) \sim t^{-\gamma}$ with $\gamma = 0.5$. If a positive bias in introduced in the system, $\gamma \approx 1$ for all $\epsilon > 0$ [14, 15]. The exponent increases as the attractive dynamics result in an increased number of annihilation. As ϵ is made negative, the number of annihilation decreases as reaction becomes less probable because of the repulsion. So, $\rho(t)$ shows a slow decay in time and can be fitted to the following form

$$\rho(t) = a/(\log t)^b, \tag{1}$$

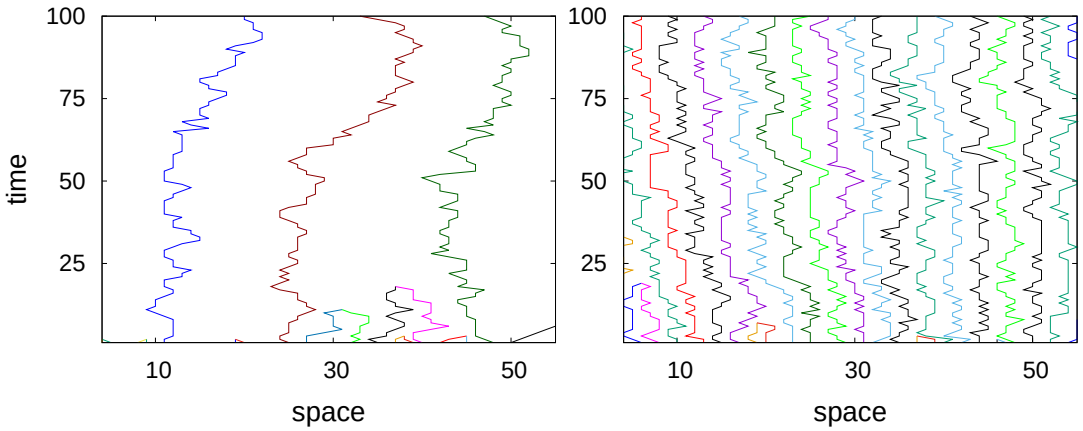


Figure 2. Snapshots of the system at different times for $\epsilon = -0.1$ (left) and $\epsilon = -0.5$ (right). The snapshots are shown for a part of a system of size $L = 200$. The trajectories of different particles are represented by different colours.

where a and b are constants, depending on ϵ. The fitting is made with a two parameter least square fitting using GNUFIT. In figure 3, $\log \rho(t)$ is plotted against $\log(\log t)$ for different ϵ values, to manifest the linear dependence at long times. Here it may be mentioned that for the extreme point $\epsilon = \epsilon_c$, the particles ideally attain a equidistant configuration. But the dynamical rule is such that the particles have to make a move and hence they perform a nearly oscillatory motion. Annihilation takes place extremely rarely at large times such that b decreases as the magnitude of ϵ increases (see inset of figure 3).

3.1.2. Persistence probability $P(t)$ Persistence probability $P(t)$ in this model is defined as the probability that a site is unvisited till time t. For $\epsilon = 0$, $P(t)$ decays as $P(t) \sim t^{-\theta}$ with $\theta = 0.375$ [19]. For $\epsilon > 0$, $\theta \approx 0.235$, however small be the bias [14]. As ϵ becomes negative, $P(t)$ falls off rapidly (see figure 4). $P(t)$ shows a stretched exponential decay in time:

$$P(t) = q_0 \exp(-qt^r). \tag{2}$$

Once again, the best fit curves with a three parameter function are obtained using GNUFIT. In figure 4 we show the validity of the above form by obtaining linear dependence when $\log(\log q_0/P(t))$ is plotted against $\log t$. Both q and r increase as $\epsilon \to \epsilon_c$.

3.2. Tagged particle features

3.2.1. Probability distribution $\Pi(x,t)$ For pure random walk ($\epsilon = 0$), the probability distribution $\Pi(x,t)$ is known to be Gaussian and $\Pi(x,t)t^{1/2}$ shows a data collapse for different times when plotted against $x/t^{1/2}$. This is also true for the unbiased ($\epsilon = 0$)

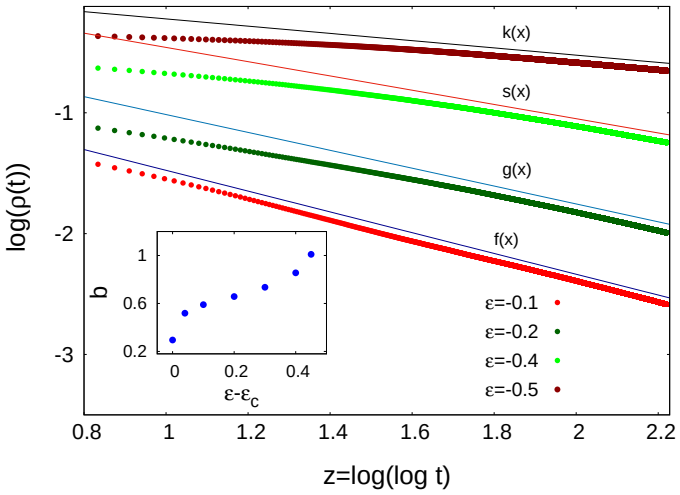


Figure 3. Variation of the fraction of surviving particles $\rho(t)$ with time t is studied by plotting $\log(\rho(t))$ against $z = \log(\log t)$ and the best fit lines (according to equation (1)) along with, shifted vertically for better visualisation. The best fit lines are (a) $f(z) = \log(0.51) - 0.86z$ for $\epsilon = -0.1$, (b) $g(z) = \log(0.7) - 0.74z$ for $\epsilon = -0.2$, (c) $s(z) = \log(1.07) - 0.59z$ for $\epsilon = -0.4$ and (d) $k(z) = \log(1.01) - 0.3z$ for $\epsilon = -0.5$. These results are for a system size $L = 8000$. Inset shows the variation of b with $\epsilon - \epsilon_c$, where $\epsilon_c = -0.5$. The errors are less than the size of the data points.

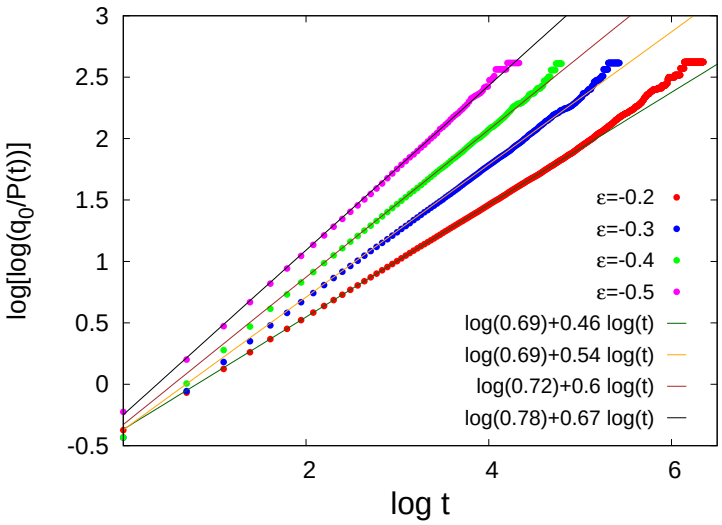


Figure 4. Variation of the persistence probability $P(t)$ with time t is studied by plotting $\log(\log \frac{q_0}{p(t)})$ against $\log t$ for several ϵ and the best fit lines (according to equation (2)) are shown along with for different ϵ in the same order. These results are for a system size $L = 8000$.

annihilating random walkers because they perform purely diffusive motion until they are annihilated. For $\epsilon < 0$, the distributions can again be fit to a Gaussian form. However the scaling variable is in general x/t^{α} with $\alpha < 0.5$. We extract the value of α from the data using two different methods.

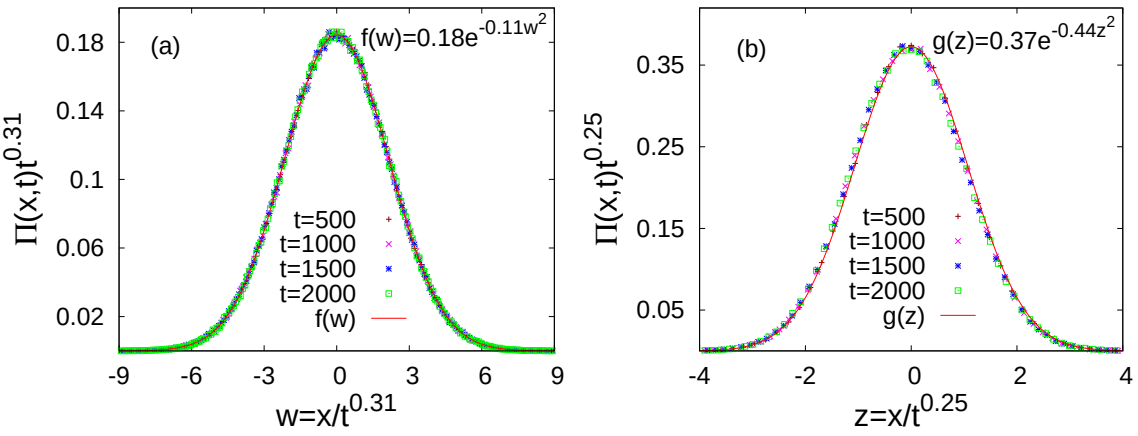


Figure 5. Data collapse of probability distribution $\Pi(x,t)$ is studied by plotting $\Pi(x,t)t^{\alpha}$ against x/t^{α} for $\epsilon = -0.1$ (a) and $\epsilon = -0.5$ (b), where $\alpha = 0.31$ for $\epsilon = -0.1$ and $\alpha = 0.25$ for $\epsilon = -0.5$, obtained using Method I for a system of size $L = 12000$. The collapsed data are fitted to the Gaussian distribution functions $f(w)$ and $g(z)$ for $\epsilon = -0.1$ and $\epsilon = -0.5$ respectively.

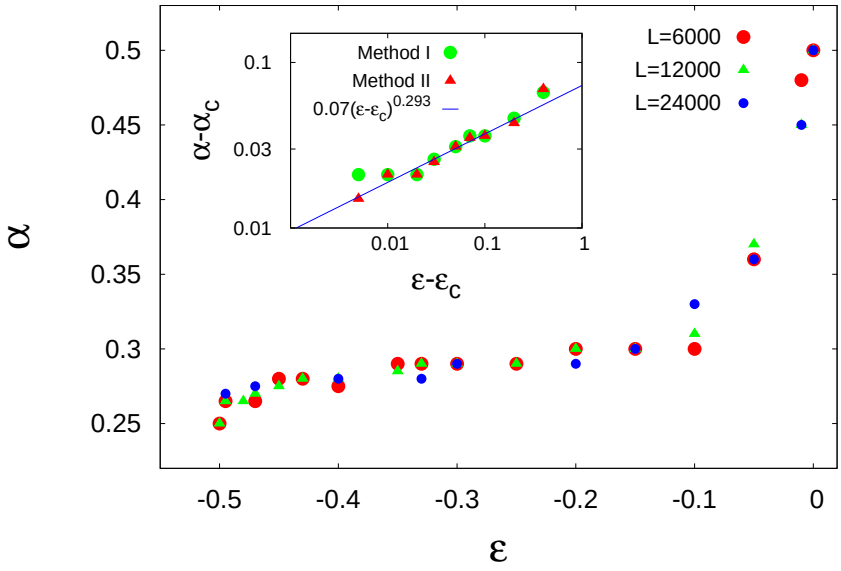


Figure 6. Variation of α is shown with ϵ for several system sizes using Method I. Inset shows $\alpha - \alpha_c$ against $\epsilon - \epsilon_c$ for Methods I and II for a system size $L = 12000$ where $\alpha_c = 0.244 \pm 0.001$ corresponds to $\epsilon = \epsilon_c = -0.5$ and a power law fitting is shown for the values obtained from Method II. The errors involved in the estimate of α from Method II is ± 0.001 while for Method I it is typically 0.005.

Method I: In this method the scaling variable α is obtained by collapsing the data using trial values of α and choosing the value for which the data collapse looks most impressive (see figure 5). This analysis indicates that α depends on ϵ, the values are shown in figure 6. There seems to be some finite size dependence which, however, could not be systematically captured in this method. As ϵ decreases from zero, at first α

decays rapidly from the value 0.5 at $\epsilon = 0$ until $\epsilon \simeq -0.1$ where it attains a value close to 0.3. Below $\epsilon = -0.1$, α shows a slow decrease and at ϵ_c, it is close to 0.25, the value expected for repulsive random walkers [20]. At large time as the walkers do not annihilate, effectively they perform repulsive random walk in the lattice. The typical error involved in the above estimates is ± 0.005.

Method II: The values of α obtained from Method I indicates that α has a comparatively weaker variation with ϵ for $\epsilon < -0.1$. To obtain a more accurate dependence of α for $\epsilon < -0.1$, we employ another method that optimises the value of α needed to obtain the best data collapse. Here we utilise the fact that the scaling function is Gaussian. Method II is based on the prescription given in [21], when the form of the scaling function is known.

For a given ϵ value, we use the same four sets of data corresponding to four different times that were used to get the collapse in Method I. We first choose a value of α and taking any of the four sets of data (say, the ith set with a probability distribution $\Pi_i(x,t)$), fit a Gaussian function to the scaled probability distribution $\Pi_i(x,t)t^\alpha$. The scaling variable here is x/t^α such that

$$\Pi_i(x,t)t^\alpha = a_i \exp[-b_i(x/t^\alpha)^2]. \tag{3}$$

Knowing a_i and b_i from the fitting, we now choose another set $j \neq i$, and estimate the deviation from the above Gaussian function by calculating

$$e_j^i = \langle \left[\left(\Pi_j(x,t)t^\alpha - a_i \exp[-b_i(x/t^\alpha)^2] \right)^2 \right] \rangle, \tag{4}$$

$\langle .... \rangle$ denotes average over all the discrete points x/t^α in the jth data set. The total averaged error for the choice of the ith set as the initial set is then equal to $E_i = \sum_{j \neq i} e_j^i/3$.

Next we repeat the above exercise by choosing a different set as the initial set to get E_i, $i = 1, 2, 3,$ and 4 and finally compute the averaged error

$$E(\alpha) = \frac{1}{4} \sum_{i=1}^{4} E_i. \tag{5}$$

Plotting $E(\alpha)$ against α, a minimum value is expected at a certain value of α which is identified as the optimal value that gives the best data collapse.

A minimum value of $E(\alpha)$ is indeed obtained as we vary the value of α in steps of 0.001. The results for $E(\alpha)$ are shown for different vales of ϵ in figure 7. The values of $\alpha - \alpha_c$ where α_c corresponds to $\epsilon = \epsilon_c$ are plotted in the inset of figure 6 obtained from both the methods and a log-log plot shows that a variation

$$\alpha - \alpha_c \propto |\epsilon_c - \epsilon|^{0.293 \pm 0.029} \tag{6}$$

is quite compatible with the more accurate estimates of Method II close to small values of $\epsilon - \epsilon_c$.

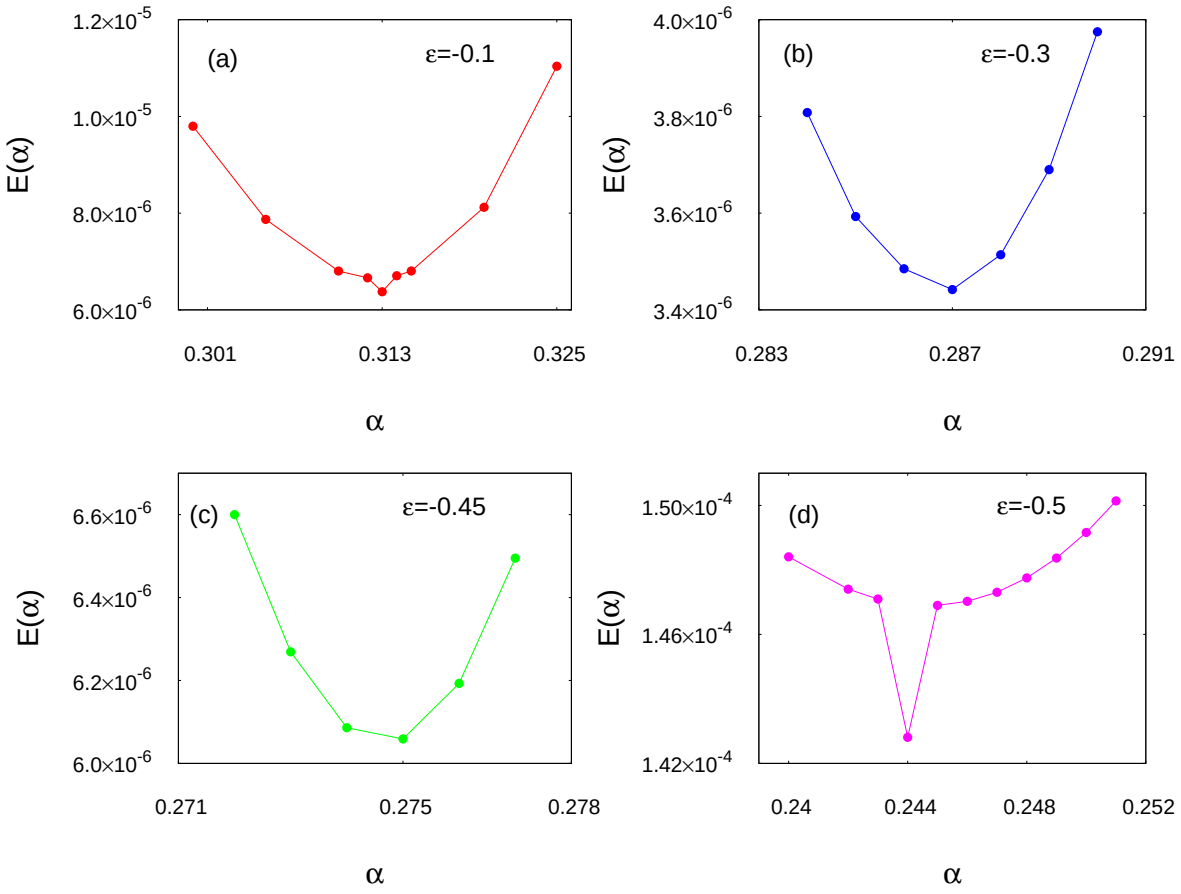


Figure 7. Variation of $E(\alpha)$ for different values of ϵ for $L = 12000$.

3.2.2. Probability of direction change $S(t)$ The probability of direction change of a particle is calculated by estimating the number of particles that changes direction of motion at time t divided by the number of surviving particles at that time. Figure 8 shows the data for $S(t)$ for different ϵ. For purely diffusive system ($\epsilon = 0$), $S(t)$ is independent of time, $S(t) = p_0$. p_0 is dependent on the dynamical updating rule, it turns out to be ~ 0.27 numerically with the asynchronous updating rule used here [16].

For $\epsilon < 0$, at first $S(t)$ increases with time, then it reaches a constant value S_{sat}. Repulsion between the neighbouring particles is mainly responsible for the change in direction of motion. When ϵ decreases from zero the repulsive factor becomes stronger, particles change their direction more rapidly, $S(t)$ increases. At the extreme limit $\epsilon = \epsilon_c$, the change in direction is maximum as the particles perform nearly oscillatory motion. A systematic decrease of the saturation value is obtained when S_{sat} (calculated from the last 500 steps) are plotted against $\epsilon - \epsilon_c$ (see inset of figure 8).

3.2.3. Distribution of time interval spent without change in direction of motion $D(\tau)$ Another quantity calculated is $D(\tau)$, the probability distribution of the interval of time τ spent in between two successive changes in direction. A particle may continue to move in

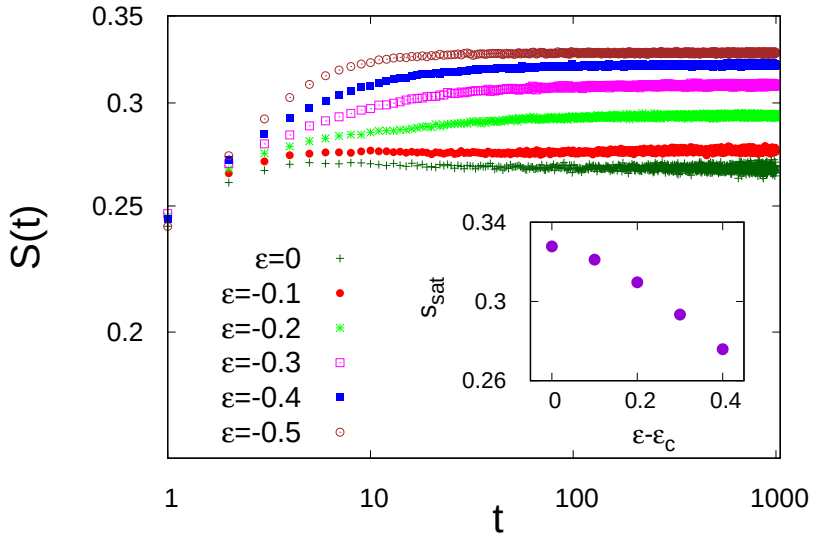


Figure 8. Probability of direction change $S(t)$ of a tagged particle at time t for different ϵ for $L = 10000$. Inset shows variation of S_{sat} with $\epsilon - \epsilon_c$. The errors are less than the size of the data points

.

the same direction for different intervals of time denoted by τ. For each tagged particle, these intervals are calculated (up to a particular time t) to obtain the distribution $D(\tau)$ at t, which is normalised such that $\sum_\tau D(\tau) = 1$. Here we have calculated $D(\tau)$ at $t = 1000$.

For random walkers with $\epsilon = 0$, $D(\tau)$ is given by

$$D(\tau) = {p_0}^2(1 - p_0)^\tau, \tag{7}$$

which reduces to an exponential form: $D(\tau) \propto \exp[-\tau \ln\{1/(1-p_0)\}]$. As for $\epsilon < 0$, $S(t)$ is a constant at large times, $D(\tau)$ is expected to show an exponential decay. Therefore, $D(\tau)$ is fitted according to

$$D(\tau) = c \exp(-d\tau). \tag{8}$$

Figure 9 shows the data for $D(\tau)$ against τ for different values of ϵ calculated at time $t = 1000$. $1/d$ is an effective 'time scale' which increases with $\epsilon - \epsilon_c$, shown in the inset of figure 9 (calculated from the tail of the distribution). It shows that for ϵ_c, the tendency to oscillate is maximum.

In principle, the value of d in equation (8) should be identical to $\ln\{1/(1 - S_{sat})\}$. In order to check this, a careful inspection of the behaviour of $D(\tau)$ shows that d has a different value for small τ (up to $\tau \approx 15$) and for the tail of the distribution. We have tabulated both the values obtained from the two regimes in Table 1 as well as the values of $\ln\{1/(1 - S_{sat})\}$ for comparison. Evidently, the values of the latter quantity match better with the d values obtained from the smaller τ region of $D(\tau)$. This may be because for larger τ, the statistics is poorer as $D(\tau)$ follows an exponential distribution. The discrepancy between the calculated value of d from S_{sat} and that from large τ region

of $D(\tau)$ increases systematically with the magnitude of ϵ which may be because we are calculating $D(\tau)$ at the same time for all ϵ.

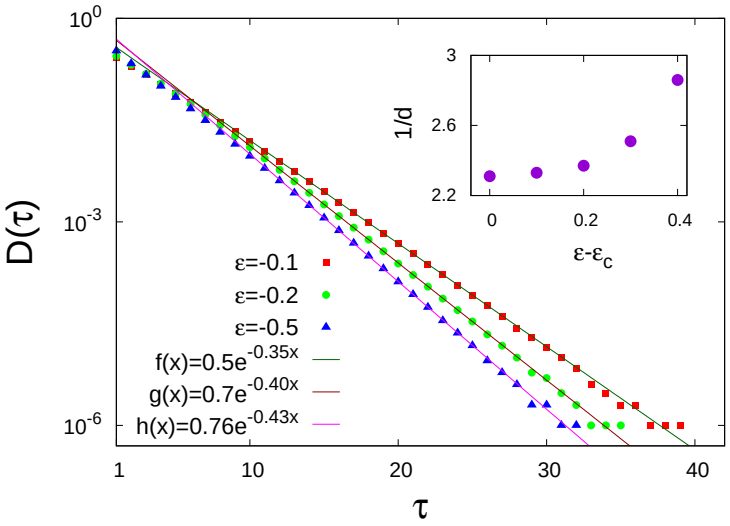


Figure 9. Variation of $D(\tau)$ over τ is studied at time $t = 1000$ and shown in a log linear plot for several ϵ. The best fit lines (according to equation (8)) are shown along with for different ϵ in the same order. Inset shows the variation of $\frac{1}{d}$ with $\epsilon - \epsilon_c$. The errors are less than the size of the data points. These results are for system size $L = 10000$.

Table 1. Comparison of d with $\ln \frac{1}{1-S_{sat}}$; typical errors are of the order of 1% for all the estimates.

ϵ	S_{sat}	$\ln \frac{1}{1-S_{sat}}$	d (for small τ)	d (for large τ)
-0.1	0.276	0.323	0.320	0.350
-0.2	0.293	0.347	0.346	0.400
-0.3	0.310	0.371	0.370	0.423
-0.4	0.321	0.387	0.383	0.430
-0.5	0.328	0.396	0.397	0.431

4. Concluding remarks

In this paper, we have studied the behaviour of the $A + A \to \emptyset$ model in one dimension, where the particles tend to avoid their nearest neighbour. The probability to move towards the nearest neighbour is taken parametrically as $0.5 + \epsilon$ where $\epsilon < 0$. The case with $\epsilon > 0$ has been studied earlier [14, 15, 16]. The bulk properties of the system show abrupt changes for any $\epsilon \neq 0$. In particular, a significant result in the present paper is that the fraction of surviving walker shows an inverse logarithmic decay for

$\epsilon < 0$. Usually we find a power law decay in one dimension with possibly a logarithmic correction, e.g., in [22] and purely logarithmic in rare cases, an example in higher than two dimensions can be found in [23].

For $\epsilon > 0$ the bulk properties (e.g., persistence probability, fraction of surviving particles) show universality in the sense there is a unique scaling behaviour of the dynamical quantities independent of ϵ. As a negative bias is incorporated in the system, both the fraction of surviving particles and persistence probability show a ϵ dependent behaviour. The persistence probability also does not show a power law dependence on time. The behaviour of the bulk properties can be qualitatively understood; the nature of the bias makes the particles more long lived and as a consequence, the probability of a site remaining unvisited decays faster than a power law.

At the microscopic level the system also shows completely different behaviour for positive and negative bias. First, the distributions have a different nature (Gaussian, single peaked) and also show a ϵ dependent scaling behaviour for the negative bias. Secondly, there is no crossover behaviour as found for the positive bias case. The negative bias case is entirely dominated by the repulsion from an early stage which causes rapid change of direction such that $S(t)$ increases as ϵ becomes more negative.

For the fully biased case, $\epsilon = \epsilon_c = -0.5$, the motion is effectively the same as the repulsive motion between random walkers [20] where the scaling behaviour is known to be $x \sim t^{1/4}$, which is also obtained from the simulations. Here we find in general $x \sim t^{\alpha}$; an interesting issue is the dependence of α on ϵ. The present results suggest that α has a weak dependence on ϵ for $\epsilon < -0.1$; it continuously decreases from ~ 0.3 to 0.25 for $-0.1 \geq \epsilon \geq -0.5$. This has been confirmed using two different methods. We also find that $\alpha - \alpha_c$ (α_c corresponds to ϵ_c) increases in a power law manner with $\epsilon - \epsilon_c$. The fact that we get $\alpha_c \simeq 0.244$ and not exactly 0.25 from Method II possibly indicates the presence of a finite size effect. On the other hand there is a sharp decay in the value of α from 0.5 to ~ 0.3 as ϵ deviates from zero.

As already mentioned, for $\epsilon > 0$, the exponents are independent of ϵ while for $\epsilon < 0$, there is a non-universality. The former case is comparable to a system of charge-less massive particles with a variable gravitational interaction between nearest neighbours, the variation arising from the diffusive component. For the latter case when $\epsilon < 0$, the system resembles a collection of like charges with variable Coulomb interaction, the diffusive component again responsible for the variation. Of course, the annihilation factor is present in both cases such that a simple mapping to a system with gravitational or Coulomb interaction is not sufficient. For $\epsilon < 0$, in the extreme limit of $\epsilon = \epsilon_c$, the diffusive component is absent and these charged particles may be regarded as electrons in a lattice perturbed from their equilibrium positions resulting in the well known oscillatory behaviour. This is because the particles attain a equidistant configuration at later times and the movements may be regarded as perturbations about their equilibrium positions.

For positive ϵ, the diffusive component does not affect the exponents and only causes a crossover behaviour while for $\epsilon < 0$, the diffusive component is more relevant

as both the bulk and tagged particle dynamics show strong ϵ dependence. Hence, in a way, the gravitational interaction appears to be more 'robust' in comparison. The reason may be related to the fact that the annihilation factor is more effective for $\epsilon > 0$; for $\epsilon < 0$, cases where the neighbours are equidistant occur more frequently, thereby enhancing the diffusive factor. This is evident from the snapshots even when ϵ is small in magnitude.

Acknowledgement: The authors thank DST-SERB project, File no. EMR/2016/005429 (Government of India) for financial support. Discussion with Purusattam Ray is also acknowledged.

5. ORCID iDs

Reshmi Roy https://orcid.org/0000-0001-6922-6858
Parongama Sen https://orcid.org/0000-0002-4641-022X

[1] Privman V., ed. *Nonequilibrium Statistical Mechanics in One Dimension*, Cambridge University Press, Cambridge (1997).
[2] Ligget T. M., *Interacting Particle Systems*, Springer-Verlag, New York, (1985).
[3] Krapivsky P. L., Redner S. and Ben-Naim E., *A Kinetic View of Statistical Physics*, Cambridge University Press, Cambridge (2009).
[4] Odor G., Rev. Mod. Phys. **76**, 663 (2004).
[5] Derrida B., J. Phys. A Math. Gen. **28**, 1481 (1995).
[6] Racz Z., Phys. Rev. lett. **55**, 1707 (1985).
[7] Amar J. G. and Family F., Phys. Rev. A **41**, 3258 (1990).
[8] ben-Avraham D., Burschka M. A., and Doering C. R., J. Stat. Phys. **60**, 695 (1990).
[9] Alcaraz F. C., Droz M., Henkel M. and Rittenberg V. , Ann. Phys. **230**, 250 (1994).
[10] Krebs K., Pfannmuller M. P., Wehefritz B. and Hinrinchsen H. , J. Stat. Phys. **78**, 1429 (1995).
[11] Santos J. E., Schutz G. M. and Stinchcombe R. B., J. Chem. Phys. **105**, 2399 (1996).
[12] Schutz G. M., Z. Phys. B **104**, 583 (1997).
[13] de Oliveira M. J., Brazilian Journal of Physics, **30** 128 (2000).
[14] Biswas S, Sen P and Ray P J. Phys.: Conf. Ser. **297**, 012003 (2011).
[15] Sen P and Ray P Phys. Rev. E **92**, 012109 (2015).
[16] Roy R, Ray P and Sen P J. Phys. A: Math. Theor. **53**, 155002 (2020).
[17] Biswas S and Sen P Phys. Rev. E **80**, 027101 (2009).
[18] Mullick P and Sen P Phys. Rev. E **99**, 052123 (2019).
[19] Derrida B, Bray A J and Godreche C J. Phys. A **27**, L357 (1994).
[20] Arratia R Ann. Probab. **11** , 362 (1983).
[21] Bhattacharjee S M and Seno F J. Phys. A: Math. Gen. **34** 6375 (2001).
[22] Dandekar R Phys. Rev E **97**, 042118 (2018).
[23] Ben-Naim E and Krapivsky P J. Phys. A **49**, 504005 (2016).